

Polyploidization in diatoms accelerates adaptation to warming

Received: 10 April 2025

Accepted: 19 September 2025

Published online: 23 October 2025

 Check for updates

Zhengke Li^{1,2}✉, Yong Zhang^{1,2,3}, Andrew J. Irwin^{1,4} & Zoe V. Finkel^{1,2}

Marine diatoms are responsible for about 20% of global primary productivity, yet their capability to adapt to long-term climate warming remains uncertain. Here we show that thermal stress induces polyploidization in the model diatom *Thalassiosira pseudonana*, and the polyploids (having more than two sets of chromosomes) adapt faster to elevated temperature compared with their diploid ancestor. Common molecular signatures underlying thermal adaptation in the polyploids included differential regulation of the cell cycle, responses to oxidative stress, cell wall biosynthesis and nutrient assimilation. Our findings indicate that polyploidization in diatoms may occur under thermal stress, triggering diverse changes in differential expression and accelerating evolutionary responses to temperature shifts. Polyploidization may be partially responsible for the past evolutionary success of diatoms and may provide an advantage to diatoms in a rapidly changing climate.

Climate change is increasing the heat content of the upper ocean, changing circulation and altering nutrient availability in the upper mixed sunlit layers of the ocean^{1–3}. In addition to changes in mean conditions, events such as marine heatwaves are expected to become more prevalent⁴. These changes are anticipated to lead to a restructuring of ocean ecosystems and a reduction in phytoplankton biomass and primary production^{5–8}. Projections of the effect of climate change generally assume phytoplankton have fixed traits, but short generation times and high levels of genetic diversity suggest phytoplankton may be able to adapt evolutionarily over years or decades^{9–17}. Consequently, predictions of ecosystem changes that ignore evolution may be misleading.

Diatoms perform about 20% of global annual primary productivity¹⁸ and thus influence the aquatic food web and are drivers of biogeochemical cycles⁵. Diatoms are very diverse¹⁹, with a wide range of genome and cell sizes; these characteristics have led to the hypothesis that genome duplication may be a key mechanism in the adaptive radiation of diatoms^{20–23} and their ability to thrive under variable environmental conditions. Polyploidy has been documented in several diatoms^{24–29} and is pervasive within higher organisms, especially plants^{30,31}. Whole-genome duplication can be stimulated by abnormal cell division in response to environmental changes such as temperature

shifts^{30,32}, which can facilitate increases in gene copy number, chromosomal distortions and genetic instability. These changes provide a molecular basis for genetic and epigenetic changes, including regulation, methylation and mutation³³ and thus may facilitate rapid adaptation to environmental change^{33,34}.

Here we exposed the diploid marine diatom *Thalassiosira pseudonana* CCMP 1335 to a range of temperatures during a short-term (~10 days) temperature performance experiment (Fig. 1a). In three experimental bottles exposed to temperatures in excess of 3 °C from the growth temperature optimum (23 °C), subpopulations of enlarged cells were observed mixed with typical-sized cells. We hypothesized these enlarged cells were tetraploids. Subcultures of these three bottles were established and maintained under slightly sub-optimal (20.0 °C) and supra-optimal (28.5 °C) growth temperatures, and over 500 generations the enlarged-cell subpopulation and median cell volume substantively increased. We quantified changes in growth rate and photophysiological traits as they may impact growth, and transcriptomic responses of the enlarged putative tetraploid lines compared with the non-enlarged diploid line, and found that polyploidization accelerates the adaptation of *Thalassiosira pseudonana* to elevated temperature.

¹School of Biological and Pharmaceutical Sciences, Shannxi University of Science and Technology, Xi'an, China. ²Department of Oceanography, Dalhousie University, Halifax, Nova Scotia, Canada. ³College of Environmental and Resource Sciences, College of Carbon Neutral Modern Industry, Fujian Key Laboratory of Pollution Control and Resource Recycling, Fujian Normal University, Fuzhou, China. ⁴Department of Mathematics and Statistics, Dalhousie University, Halifax, Nova Scotia, Canada. ✉e-mail: zkli@dal.ca

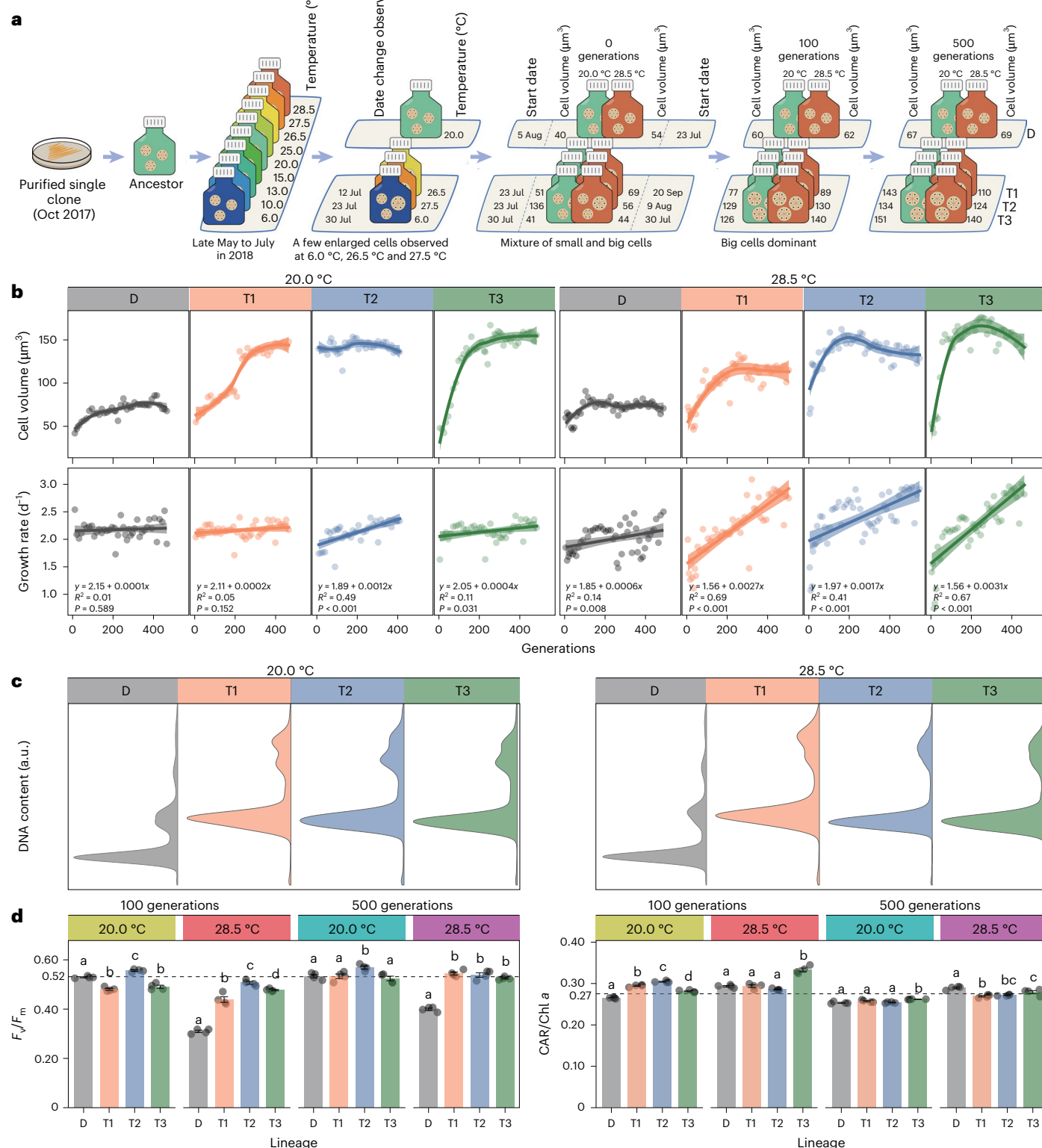


Fig. 1 | The physiological change of *Thalassiosira pseudonana* lineages after 100 and 500 generations of temperature selection (20.0 °C and 28.5 °C).

a. The experimental set-up. **b.** The cell volume and growth rate change. The cell volume and growth rate data across generations are shown with fitted lines using the 'loess' and 'glm' models, respectively, with shaded areas indicating 95% confidence intervals. **c.** The relative DNA content of the different lineages after 500 generations of temperature selection. **d.** The maximum quantum yield of PSII photochemistry, defined as the ratio of variable fluorescence ($F_v = F_m - F_0$)

to maximum fluorescence (F_m) (F_v/F_m), and the CAR/Chl α (the carotenoid to chlorophyll α ratio). Bars with different superscript letters for each combination of generation and temperature treatment indicate significant differences (one-way analysis of variance with two-sided Tukey's honestly significant difference, $P < 0.05$). Data are means \pm s.d. ($n = 4$ biological replicates). The horizontal dashed line is the value for the ancestral lineage at 20.0 °C. a.u., arbitrary units; D, diploid control line; T1, tetraploid lineage 1; T2, tetraploid lineage 2; T3, tetraploid lineage 3.

Cell volume, growth rate and DNA content change

A schematic diagram of the experimental set-up is shown in Fig. 1a. Cell volume of the diploid line (D) was stable ($40\text{--}70 \mu\text{m}^3$), while the lines with tetraploids (T1–T3) increased in median cell volume over 500 generations to between 110 and $151 \mu\text{m}^3$ under both 20.0°C and 28.5°C (Fig. 1b). Most of the temporal variation in cell volume in the tetraploid lines was associated with increases in the proportion of the enlarged population; additional variability may be attributed to the proportion of the culture in different phases of the cell division cycle (G1 versus G2) when sampled, new chromosome duplication and loss events, and measurement error. The cell division rates of the tetraploids remained similar, or even faster, than those of the D line (Fig. 1b and Extended Data Fig. 1). At 500 generations, the T1–T3 lines had approximately double the genome size of D under both temperature treatments, as measured by flow cytometry, indicating polyploidization (Fig. 1c). On the basis of these results, we infer the D line was diploid and the enlarged cells in the T1, T2 and T3 lines were tetraploid.

Evolution of photophysiology and thermal reaction norms

The maximum quantum yield of photosystem II (PSII), expressed as the ratio of variable (F_v) to maximum (F_m) fluorescence (F_v/F_m), initially decreased under 28.5°C relative to 20.0°C , but the reduction was mitigated in D and eliminated in T1–T3 at 500 generations (Fig. 1d). Pigment ratios (carotenoids/chlorophyll α and chlorophyll c /chlorophyll α) remained relatively constant over time, lineages and treatments (Fig. 1d); additional photophysiological traits are summarized in Extended Data Fig. 2. Under 20.0°C , the thermal reaction norms varied among T1–T3 (Fig. 2 and Supplementary Fig. 1). Under 28.5°C , the thermal reaction norms of T1–T3 converged, with higher growth rates and an increased optimal growth temperature of $\sim 26^\circ\text{C}$ relative to the D lineage. The D lineage had a wider thermal reaction norm than the tetraploids, and its optimal growth temperature increased $\sim 2^\circ\text{C}$ compared with the ancestral population after 500 generations (Fig. 2 and Supplementary Fig. 1).

Evolution of competitive ability

The polyploid lineages had superior relative competitive fitness under our growth conditions, particularly after long-term (500 generations) adaptation to warming (28.5°C treatment). In competition experiments conducted after 100 generations at 28.5°C , larger cells came to dominate each co-culture within 30–45 generations at 28.5°C , while the time required for their dominance was >60 generations at 20.0°C (Fig. 3a). After 500 generations at 28.5°C , no smaller cells were detected after 10 generations in co-culture when the populations were initially mixed at a 1/1 ratio. When this initial ratio was changed to 10/1 (smaller cells/larger cells), fewer than 20 generations were required for the larger cells to dominate. The number of generations required for larger cells to dominate was much longer (150–200 generations) for lineages from the 20.0°C selection treatments. At 100 generations, T2 and T3 displayed relative competitive fitness values between 1.0 and 1.1 under 20.0°C and exceeded 1.1 under 28.5°C (Fig. 3b). After 500 generations, all polyploid lineages exhibited relative competitive fitness values between 1.0 and 1.1 under 20.0°C , while reaching >1.5 (T2 and T3) or >1.75 (T1) under 28.5°C .

Evolution of gene expression and metabolic pathways

Temperature, the number of generations and ploidy were all important factors affecting gene expression (Fig. 4a). About one-third of the 11,672 genes in *T. pseudonanna* were differentially expressed between the polyploids and diploid lineages (Fig. 4b). The median absolute \log_2 fold change ($|\log_2\text{FC}|$) for differentially expressed genes (DEGs) was greater at 28.5°C compared with 20.0°C after both 100 and 500 generations, exceeding 0.7 at 28.5°C (500 generations) compared

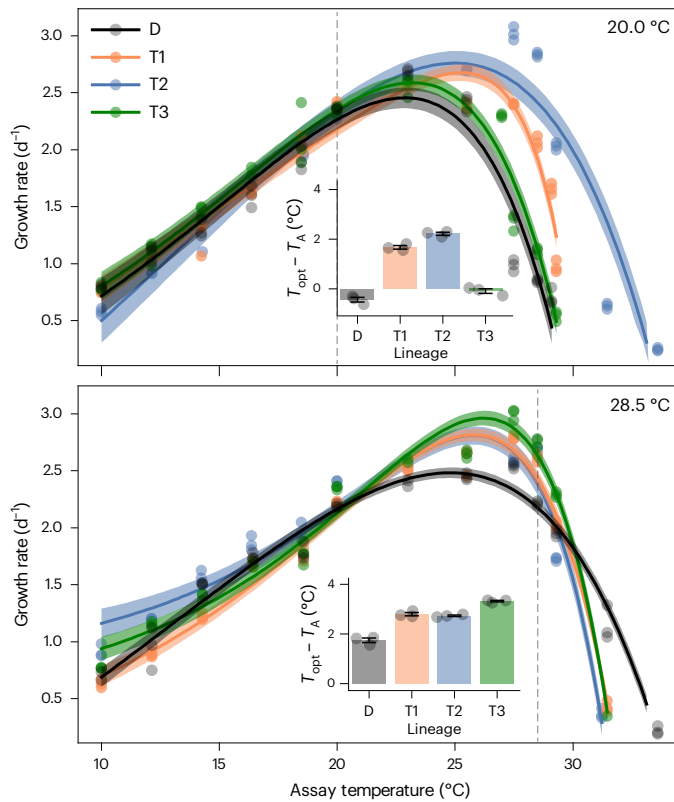


Fig. 2 | Thermal reaction norms of different *Thalassiosira pseudonanna* lineages after 500 generations of temperature selection (20.0°C and 28.5°C). The inset bar plots show the increase in optimal growth temperature relative to the ancestral lineage ($T_{0pt} - T_A$), where T_{0pt} is the optimal growth temperature of each lineage (D, T1, T2, T3) and $T_A = 23.3^\circ\text{C}$ is the optimal temperature of the ancestor. Each dot represents one of $n = 3$ biological replicates. The dashed vertical lines indicate the corresponding growth rates observed at these experimental temperatures. The thermal reaction norm of the ancestor is provided in Supplementary Fig. 1. Growth rates were measured in triplicate (dots) at assay temperatures.

with <0.5 in other treatments (Fig. 4b and Supplementary Fig. 2). Many DEGs for each temperature treatment and number of generations were lineage-specific (Fig. 4c), with only eight sets of up- or down-regulated genes common across T1–T3, termed polyploid DEGs (pDEGs; Fig. 4c (highlighted in pink) and Supplementary Dataset 3).

A gene ontology biological process (GO-bp) enrichment analysis on the pDEGs at each temperature and number of generations showed that most GO-bp terms were enriched in pDEGs in only one of the four treatments (Fig. 5a). The main exception was the enrichment of terms associated with the down-regulation of regulation processes after 500 generations in both temperature treatments. We identified 23–143 pDEGs shared across the same temperature at different numbers of generations or across the same number of generations and different temperatures (Fig. 5b (numbers in open circles) and Supplementary Dataset 5). Significantly enriched GO-bp terms were found in only two of these contrasts. At 500 generations, down-regulated genes in the polyploids were enriched in terms associated with seven regulatory processes, mitotic cell-cycle phase transition, two modification processes and two cell-wall-related processes (Fig. 5b). At 28.5°C , down-regulated genes showed significant enrichment in late endosome to vacuole transport, nucleosome assembly, cellular and macromolecule localization, two autophagy-related processes and intracellular iron ion homeostasis (Fig. 5b). Only three up-regulated genes (*THAPSDRAFT_12116*, encoding a HSF_DOMAIN-containing protein; *THAPSDRAFT_37357*, encoding Histone H4; *THAPSDRAFT_25801*) and

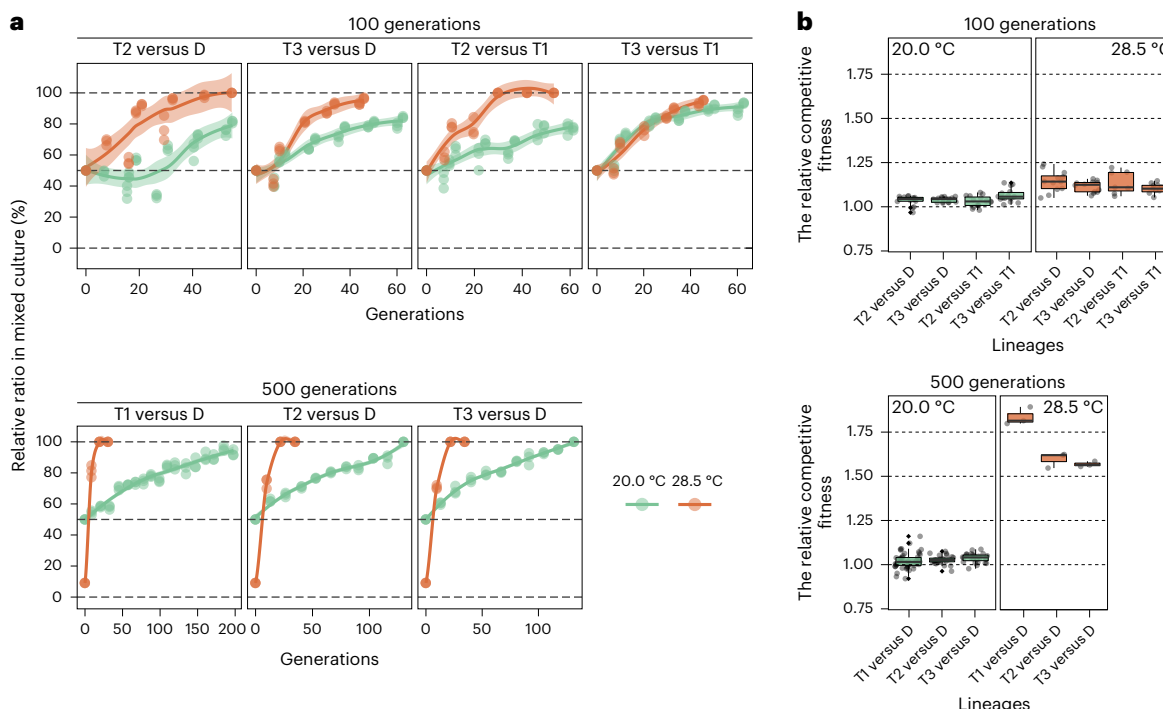


Fig. 3 | The competitive ability of the tetraploid *Thalassiosira pseudonana* lineages after 100 and 500 generations of temperature selection (20.0 °C and 28.5 °C). **a**, The panels show competition experiments started after 100 (top) and 500 (bottom) generations of temperature selection. Each sub-panel shows the proportion of the larger lineage in each competition experiment. Each dot represents one of $n = 3$ biological replicates. **b**, The relative competitive fitness of the larger lineages. Box plots show medians (centre lines), interquartile range (boxes, 25–75%), whiskers ($1.5 \times$ interquartile range) and outliers (black diamonds). Each independent inoculation was performed with three biological replicates. Depending on the condition, 1–17 consecutive inoculations were conducted, yielding $n = 3$ –51 data points,

which are shown as dots in the figures. The relative competitive fitness was calculated by determining the ratio of growth rates between pairs of lineages in each competition experiment. Although the Coulter counter provided reliable monitoring of relative population sizes for each lineage, the convergence of cell volumes between T1 and D lineages at 100 generations prevented unambiguous discrimination between these populations. Consequently, competitive co-culture experiments between these particular lineages were not conducted at 100 generations. The competition experiments were conducted at each lineage's respective cultivation temperatures (20.0 °C and 28.5 °C). The generations were calculated on the basis of the total cell density of both lineages within the competition experiments.

four down-regulated genes (*THAPSDRAFT_22846*, encoding a Methyltransf_21 domain-containing protein; *THAPSDRAFT_3250*; *THAPSDRAFT_14899*; *THAPSDRAFT_21665*) were differentially expressed in the same direction for all treatments and tetraploid lineages.

Heat maps for genes within the enriched GO-bp terms (Fig. 5a,b) and additional related processes reveal an intensification in the magnitude and count of DEGs in three polyploids under 28.5 °C, with the most pronounced effects at 500 generations (Supplementary Figs. 3–18). At 500 generations under 28.5 °C, key transport genes up-regulated in two to three polyploid lines include nitrogen transporters (for example, *NRT* and some *AMT*), phosphate transporters (for example, *IPT*, *NPT* and *alkaline phosphatase*), high-affinity iron transporters (for example, *FTR*) and a zinc transporter (*ZntA*). By contrast, silicic acid transporters (for example, *SIT2* and *SIT3*) and copper transporters were predominantly down-regulated (Supplementary Figs. 3 and 4). Several genes associated with potassium ion transport, late endosome to vacuole transport, and intracellular iron ion homoeostasis were down-regulated, while amino acid and organic acid transmembrane transport were up-regulated in 2–3 polyploids exposed to 28.5 °C for 500 generations (Supplementary Figs. 5–7).

Many genes involved in DNA replication and elongation were significantly up-regulated in most polyploid lineages at 500 generations, particularly under 28.5 °C (Supplementary Fig. 8). Histone genes displayed divergent expression: *H1.5*, *H2A* and *H2B* genes were broadly up-regulated while most *H3* and *H4* genes were down-regulated, especially under 28.5 °C at 500 generations (Supplementary Figs. 8 and 9). Cell-cycle-related genes (for example, *ERK*, *CDC6* and several

MCM complex members) were strongly up-regulated under 28.5 °C, particularly at 500 generations (Supplementary Fig. 10), whereas cyclin-dependent protein kinase genes (for example, *CDC28* and *CDK10*) were down-regulated exclusively under 28.5 °C at 500 generations. Many diatom-specific cyclin³⁵ and non-diatom-specific cyclin (for example, *cyclin E1*) genes exhibited widespread down-regulation, while a subset (for example, *A/B cyclins*) were specifically up-regulated under 28.5 °C at 500 generations (Supplementary Fig. 10).

Many genes related to chitin metabolism and cell-wall organization or biogenesis (for example, chitinase, chitin synthase and chitodextrinase) were predominantly down-regulated under 28.5 °C at both 100 and 500 generation (Supplementary Figs. 11 and 12). Several genes associated with response to stress/stimulus exhibit differential expression, particularly under 28.5 °C at 500 generations. Detoxification/redox-related genes (for example, *GSR*, *GST*, aldo-keto oxidoreductase and dehydrogenase) were up-regulated while stress response genes (for example, aldo-keto reductase, *HSPs*, *SOD*, haem oxygenase and several proteasome genes) were down-regulated in at least two out of the three polyploids under 28 °C at the 500 generations (Supplementary Figs. 13 and 14).

Discussion

Diatoms are a speciose and ecologically important group of phytoplankton characterized by a large range of cell and genome sizes^{20,36}. Their evolutionary radiation and ecological success mirror those of flowering plants, and both appear to have exploited the advantages of polyploidization to achieve their evolutionary success^{21,31}.

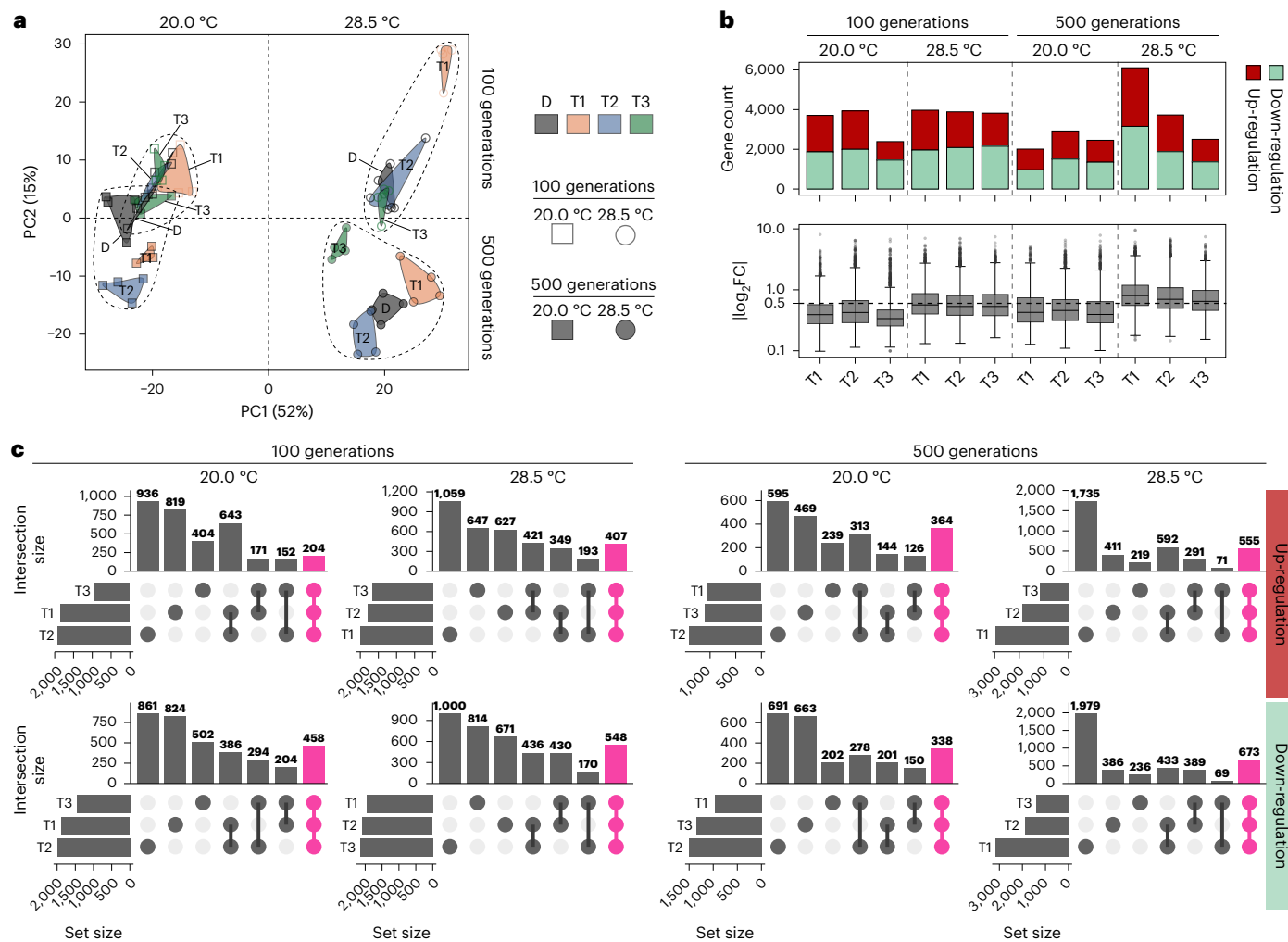


Fig. 4 | Gene expression analysis in four *Thalassiosira pseudonana* lineages after 100 and 500 generations of temperature selection (20.0 °C and 28.5 °C). **a**, Principal component analysis of variance-stabilizing transformed count data. The dashed irregular ovals were drawn to highlight samples under different treatments (generations \times temperatures). Vertical and horizontal dashed lines divide the principal component analysis plot along PC1 and PC2, aiding comparison samples between different treatments. **b**, The gene count

and $|\log_2\text{FC}|$ of the DEGs. Box plots show median (centre line), interquartile range (box, 25–75%), whiskers ($1.5 \times$ interquartile range) and outliers (light-grey dots). The P values from the two-sided Mann–Whitney U test comparing the $|\log_2\text{FC}|$ values of the polypliod lineage across different treatments are presented in Supplementary Fig. 2. **c**, Upset plot enumerating DEGs found in one or more of the three polypliod lineages. pDEGs are highlighted in pink.

The documented cases of polypliodization in diverse diatom species under laboratory and field conditions^{21,24,29} and our incidental isolation of three polypliod lines of *T. pseudonana* from a temperature performance experiment suggest that polypliodization may be relatively frequent in diatoms when challenged by environmental stressors. Here we compared the polypliod with diploid response in cell physiology, fitness and gene expression to 500 generations of exposure to a very slightly sub-optimal and a supra-optimal growth temperature. Our long-term selection experiment revealed that polypliod lineages exhibited accelerated increases in absolute growth rates (Fig. 1) and relative competitive fitness (Fig. 3), supporting the hypothesis that polypliodization enables more rapid adaptation to elevated temperature, and polypliodization may be an underappreciated strategy used by diatoms in their response to environmental change.

The doubling of ploidy in *T. pseudonana* was associated with a near doubling of cell volume (Fig. 1 and Table 1). In yeast, cell volume increases approximately linearly with ploidy, and cell division rate is often maintained or slightly reduced with higher ploidy³⁷. In *T. pseudonana*, cell division rates, cellular chlorophyll concentration ($\text{Chl } a \mu\text{m}^{-3}$), and $\text{Chl } c/\text{Chl } a$ and carotenoid/Chl a ratios did not

systematically respond to cell-volume doubling. These findings parallel observations in *D. brightwellii* cultures with varying cell volume, but contrast with differences between its genome-size variants (putative cryptic species)^{29,38}. Notably, $\text{Chl } a \mu\text{m}^{-3}$ was elevated at 28 °C versus 20.0 °C, and cell division rates increased markedly in all the polypliods exposed to high growth temperature after 500 generations (Fig. 1 and Extended Data Fig. 2). The higher growth rate in the polypliod lines led to greater relative competitive fitness than the diploid line under both 20.0 and 28.5 °C, despite non-significant measured differences in growth rate between the diploid and some of the polypliod lines at 20.0 °C (Fig. 3). The three polypliod lines exhibited predictable changes in genome size and cell volume and similar temporal trajectories in growth rate and photosynthetic traits, but physiological changes and differential gene expression varied across the polypliod lineages and time (Fig. 4), leading to distinct evolutionary trajectories.

It is often assumed that selection pressure for higher growth rates at elevated temperatures may lead to a narrowing of the range of tolerated temperatures⁹. After 500 generations at 28.5 °C, the polypliod lines all exhibited an upward shift in maximum growth rate and optimal growth temperature and a narrowing in the range of viable growth

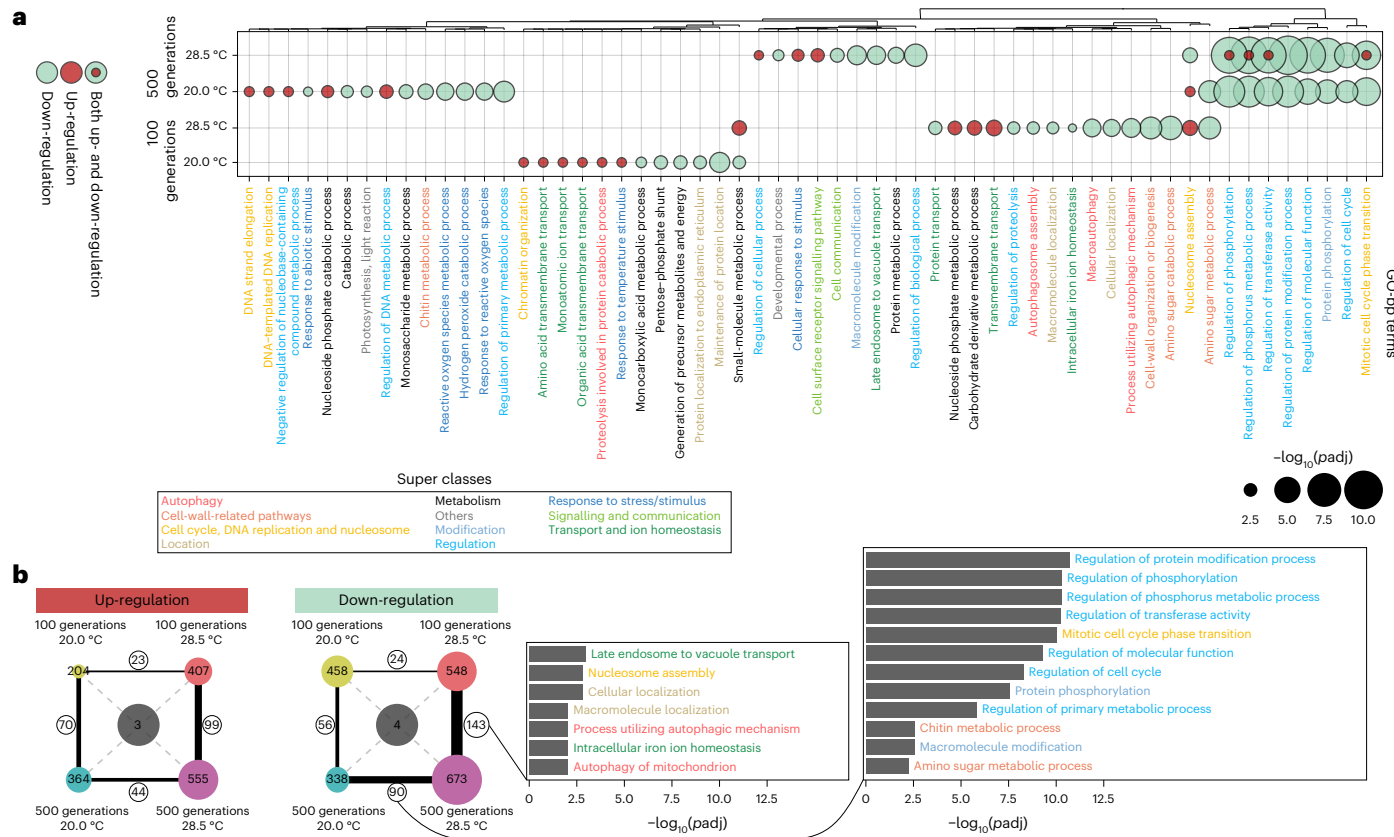


Fig. 5 | Functional enrichment of pDEGs. **a**, GO-bp enrichment with REVIGO analysis of the pDEGs. **b**, Gene count and the GO-bp enrichment with REVIGO analysis of the pDEGs across temperatures or generations. The lines connecting pairs of treatments indicate the common pDEGs shared between those treatments. Note that there were only two pairs of treatments (28.5 °C for 500 generations versus 20.0 °C for 500 generations; 28.5 °C for 500 generations versus 28.5 °C for 100 generations) that have common pDEGs enriched in GO-bp terms. The line thickness and circled number indicate the count of the overlapping pDEGs. The colour-filled circles represent the pDEGs specific to each treatment. The grey open circles and the numbers on them, located

on the cross-dashed lines, represent the count of pDEGs shared across all four treatments. REVIGO web service was used to remove redundant and similar GO-bp terms resulting in a smaller number of categories by semantic clustering. Closely related GO-bp terms were manually classified into ‘super classes’ to aid visualization. The super classes and their GO-bp terms are shown in Supplementary Dataset 4. The pDEGs and their annotations are shown in Supplementary Dataset 3, and the common pDEGs and their annotations are shown in Supplementary Dataset 5. GO enrichment was tested with a one-sided hypergeometric test with P values adjusted by the Benjamini–Hochberg method. p_{adj} , adjusted P value.

Table 1 | The median cell volume (μm^3) of four size-defined phenotype lines of *Thalassiosira pseudonana* after 0, 100 and 500 generations of temperature selection (20.0 °C and 28.5 °C)

| Temperature (°C) | Phenotype line | 0 generation | 100 generations | 500 generations |
|------------------|----------------|--------------|-----------------|-----------------|
| 20.0 | D | 40 | 60 | 67 |
| | T1 | 51 | 77 | 143 |
| | T2 | 136 | 129 | 134 |
| | T3 | 41 | 126 | 151 |
| 28.5 | D | 54 | 62 | 69 |
| | T1 | 69 | 89 | 110 |
| | T2 | 56 | 130 | 124 |
| | T3 | 44 | 140 | 140 |

temperatures relative to the diploid line. These findings suggest polyploidization may promote specialization at the expense of environmental versatility³⁴. By contrast, after 500 generations under 20.0 °C, there was little change in the maximum growth rate of the diploid line

and one of the polyploid lineages (T3) while the two polyploid lineages (T1 and T2; Fig. 2) that exhibited increases in their optimal growth temperature had the widest range of tolerated temperatures. These results suggest it may be difficult to make predictions about evolutionary changes in temperature performance, although the trade-off might develop under 20.0 °C with a longer selection experiment. Growth rates changed throughout the 500 generations in most lines, with the most rapid changes observed in the polyploid lines exposed to elevated temperature. Compared with the ancestral growth rate of the diploid line at 20.0 °C ($\mu = 2.15 \text{ d}^{-1}$), after 500 generations we observed a 37% increase in growth rate of the polyploids at 28.5 °C. Growth rates were still increasing at the end of the experiment, which comports with a predicted potential growth rate increase due to the temperature change predicted by the Eppley model³⁹ of 71% in the 28.5 °C treatment ($= 1.88^{(8.5/10)} - 1$).

The mechanisms through which polyploidization impacts gene expression and the ability to adapt to new conditions in diatoms remain poorly understood. In yeast and human tumour cells, a doubling of chromosomes (autopolyploidy) is typically associated with an increase in mRNA, but in the short term there is relatively little change in gene expression or protein content^{37,40–43}. Over the longer term, duplicated genes may provide substrate for novel mutations, increasing genetic diversity and heterozygosity^{33,44}, and epigenetic changes and

chromosome loss are possible in both the short and longer term^{45,46} and may be responsible for some of the variability in cell volume in the cultured lineages over time (Fig. 1b). In *T. pseudonana* we find only seven DEGs in common across all the polyploids (pDEGs) relative to the diploid line at both experimental temperatures and the two generation times examined (Fig. 5b). A closer look at the differential regulation of genes and pathways associated with the identified polyploid-specific enriched biological processes (Supplementary Figs. 3–18) suggests widespread DEGs associated with the cell wall and silicification, and histones and the cell division cycle and its regulation. There is a larger set of pDEGs associated with elevated temperature and the largest increases in growth rate, especially after 500 generations; these genes are associated with nutrient uptake, transmembrane transport, some additional aspects of DNA replication and elongation, nucleosome assembly and the cell cycle, and responses to reactive oxygen species and other stressors. We speculate that it is these genes that may be responsible for the higher cell division rate and competitive ability of the polyploids under elevated temperature.

While ploidy-dependent changes in phenotype and gene regulation may be beneficial for polyploids under some environmental conditions, they may be disadvantageous under others⁴⁷. In general, smaller cell volumes are advantageous for phytoplankton under lower nutrient regimes because their higher surface area-to-volume ratios support a higher diffusive supply of nutrient per unit cell volume. While polyploidization increases the fitness of the marine diatom *T. pseudonana* to elevated temperature, we recognize that this response may be species specific, possibly facilitated by the potential loss of sexual reproduction in this species⁴⁸. Moreover, increases in ocean temperatures are expected to increase vertical stratification and reduce inorganic nutrient supply over vast areas of the ocean surface, and therefore increases in cell volume could be disadvantageous. In some plants, polyploidy is associated with increased nutrient uptake and nutrient concentrations^{49,50}. In the diatom *T. pseudonana*, polyploidy is associated with the up-regulation of several nitrogen and phosphorus uptake-related genes (Supplementary Figs. 3–7). The up-regulation of nutrient metabolism, especially nitrogen and phosphate, could provide the elevated nutrient supply required to support higher growth rates, especially under elevated temperature. By contrast, genes associated with silicon metabolism, the cell wall and chitin are predominantly down-regulated, especially under elevated temperature (Supplementary Figs. 4, 11 and 12). *Thalassiosira* has an absolute requirement for silicon and produces long chitin fibres that extend through the silicon wall⁵¹. The down-regulation of silicon and chitin metabolism in the polyploids may be due to the relative decrease in surface area/cell volume and increase in growth rate⁵² under elevated temperatures, which in aggregate may act to decrease cellular silicon requirements.

Polyploids often experience challenges in chromosome segregation during mitosis and meiosis, which can lead to genome instability, including loss of DNA, partial or whole chromosomes, and genome reorganization⁵³. Regulatory changes may be required for successful chromosome assortment and segregation for polyploid persistence after whole-genome duplication⁵⁴. In *T. pseudonana* the polyploid lineages are enriched in differentially expressed genes in cell cycle, DNA replication and nucleosome and regulatory categories (Fig. 5a,b and Supplementary Figs. 8–10). More specifically, in the 28.5 °C treatments there is an up-regulation of genes associated with DNA replication, DNA strand elongation and an intriguing pattern of differential regulation of histones and cyclins. There is a common decrease in gene expression across the polyploids associated with a set of 16 diatom-specific cyclins, many of which are expressed during the G1-to-S phase³⁵. There is a second set of cell-cycle genes that are up-regulated, primarily under 28.5 °C and after 500 generations, that includes a subset of diatom cyclins, kinases and cell division control proteins. Similarly, there is a set of histones—H1/S, H2A/B, H3 and H4—that are generally up-regulated

and another set that are down-regulated: H3 and H4, especially in the 28.5 °C treatment. The down-regulation of G1/S diatom-specific cyclins and up-regulation of G2/M-regulation of cyclins and cyclin A may act to slow the progression of the G1/S phase, promoting quality control during DNA replication, facilitating genomic stability and accelerating the later stages of the cell cycle, effectively shortening the cell cycle in the polyploids. In aggregate, this evidence suggests that the ubiquity of diatom polyploidy may be facilitated by changes in histone and cell-cycle regulation and the expanded family of diatom cyclin genes³⁵.

We hypothesize that polyploidization may be readily induced in diatoms, creating opportunities for adaptation to new environments and increases in relative fitness. The increased genetic potential associated with polyploidization in *T. pseudonana* alters differential expression across a wide variety of pathways, including regulation, cell cycle, cyclins, kinases and nutrient uptake. The impact of polyploidization unfolds over hundreds of generations with distinct responses seen over time and across different genome duplication events. Taken together, this experimental evidence suggests that polyploidization may be an important mechanism supporting the evolutionary success of diatoms, probably contributing to the diversification and radiation of this important group.

Online content

Any methods, additional references, Nature Portfolio reporting summaries, source data, extended data, supplementary information, acknowledgements, peer review information; details of author contributions and competing interests; and statements of data and code availability are available at <https://doi.org/10.1038/s41558-025-02464-1>.

References

1. Moore, J. K. et al. Sustained climate warming drives declining marine biological productivity. *Science* **359**, 1139–1143 (2018).
2. Raftery, A. E., Zimmer, A., Frierson, D. M., Startz, R. & Liu, P. Less than 2 °C warming by 2100 unlikely. *Nat. Clim. Change* **7**, 637–641 (2017).
3. Gille, S. T. Decadal-scale temperature trends in the Southern Hemisphere ocean. *J. Clim.* **21**, 4749–4765 (2008).
4. Fox-Kemper, B. et al. in *Climate Change 2021: The Physical Science Basis* (eds P. Zhai, P. & Pirani, A.) Ch. 9 (Cambridge Univ. Press, 2021).
5. Tréguer, P. et al. Influence of diatom diversity on the ocean biological carbon pump. *Nat. Geosci.* **11**, 27–37 (2018).
6. Kwiatkowski, L. et al. Twenty-first century ocean warming, acidification, deoxygenation, and upper-ocean nutrient and primary production decline from CMIP6 model projections. *Biogeosciences* **17**, 3439–3470 (2020).
7. Bopp, L. et al. Multiple stressors of ocean ecosystems in the 21st century: projections with CMIP5 models. *Biogeosciences* **10**, 6225–6245 (2013).
8. Thomas, M. K., Kremer, C. T., Klausmeier, C. A. & Litchman, E. A global pattern of thermal adaptation in marine phytoplankton. *Science* **338**, 1085–1088 (2012).
9. O'Donnell, D. R. et al. Rapid thermal adaptation in a marine diatom reveals constraints and trade-offs. *Glob. Change Biol.* **24**, 4554–4565 (2018).
10. Schaum, C. E., Buckling, A., Smirnoff, N., Studholme, D. J. & Yvon-Durocher, G. Environmental fluctuations accelerate molecular evolution of thermal tolerance in a marine diatom. *Nat. Commun.* **9**, 1719 (2018).
11. Barton, S. et al. Evolutionary temperature compensation of carbon fixation in marine phytoplankton. *Ecol. Lett.* **23**, 722–733 (2020).
12. Zhong, J. et al. Adaptation of a marine diatom to ocean acidification and warming reveals constraints and trade-offs. *Sci. Total Environ.* **771**, 145167 (2021).

13. Cheng, L. et al. Metabolic adaptation of a globally important diatom following 700 generations of selection under a warmer temperature. *Environ. Sci. Technol.* **56**, 5247–5255 (2022).
14. Jin, P. et al. Increased genetic diversity loss and genetic differentiation in a model marine diatom adapted to ocean warming compared to high CO₂. *ISME J.* **16**, 2587–2598 (2022).
15. Hattich, G. S. I. et al. Temperature optima of a natural diatom population increases as global warming proceeds. *Nat. Clim. Change* **14**, 518–525 (2024).
16. Zhou, Y. et al. The adaptive mechanisms of the marine diatom *Thalassiosira weissflogii* to long-term high CO₂ and warming. *Plant J.* **119**, 2001–2020 (2024).
17. Cheng, L., Xu, X., Wang, M. & Wang, D. Rapid adaption but genetic diversity loss of a globally distributed diatom in the warmer ocean. *Glob. Change Biol.* **30**, e17602 (2024).
18. Field, C. B., Behrenfeld, M. J., Randerson, J. T. & Falkowski, P. Primary production of the biosphere: integrating terrestrial and oceanic components. *Science* **281**, 237–240 (1998).
19. Malviya, S. et al. Insights into global diatom distribution and diversity in the world's ocean. *Proc. Natl Acad. Sci. USA* **113**, E1516–E1525 (2016).
20. Connolly, J. A. et al. Correlated evolution of genome size and cell volume in diatoms (Bacillariophyceae). *J. Phycol.* **44**, 124–131 (2008).
21. Parks, M. B., Nakov, T., Ruck, E. C., Wickett, N. J. & Alverson, A. J. Phylogenomics reveals an extensive history of genome duplication in diatoms (Bacillariophyta). *Am. J. Bot.* **105**, 330–347 (2018).
22. Mann, D. G. The species concept in diatoms. *Phycologia* **38**, 437–495 (1999).
23. Mock, T. et al. in *The Molecular Life of Diatoms* 1st edn (eds Falciatore A. & Mock T.) 111–145 (Springer, 2022).
24. Von Dassow, P., Petersen, T. W., Chepurnov, V. A. & Armbrust, E. V. Inter- and intraspecific relationships between nuclear DNA content and cell size in selected members of the centric diatom genus *Thalassiosira* (Bacillariophyceae). *J. Phycol.* **44**, 335–349 (2008).
25. Mann, D. G. & Stickle, A. J. The genus *Craticula*. *Diatom Res.* **6**, 79–107 (1991).
26. Mann, D. G. Auxospore formation, reproductive plasticity and cell structure in *Navicula ulvacea* and the resurrection of the genus *Dickieia* (Bacillariophyta). *Eur. J. Phycol.* **29**, 141–157 (1994).
27. Chepurnov, V. A. & Roschin, A. M. Inbreeding influence on sexual reproduction of *Achnanthes longipes* Ag. (Bacillariophyta). *Diatom Res.* **10**, 21–29 (1995).
28. Chepurnov, V. A., Mann, D. G., Vyverman, W., Sabbe, K. & Danielidis, D. B. Sexual reproduction, mating system, and protoplast dynamics of *Seminavis* (Bacillariophyceae). *J. Phycol.* **38**, 1004–1019 (2002).
29. Koester, J. A., Swalwell, J. E., Von Dassow, P. & Armbrust, E. V. Genome size differentiates co-occurring populations of the planktonic diatom *Ditylum brightwellii* (Bacillariophyta). *BMC Evol. Biol.* **10**, 1 (2010).
30. Mable, B. K., Alexandrou, M. A. & Taylor, M. I. Genome duplication in amphibians and fish: an extended synthesis. *J. Zool.* **284**, 151–182 (2011).
31. Otto, S. P. & Whitton, J. Polyploid incidence and evolution. *Annu. Rev. Genet.* **34**, 401–437 (2000).
32. Kreiner, J. M., Kron, P. & Husband, B. C. Frequency and maintenance of unreduced gametes in natural plant populations: associations with reproductive mode, life history and genome size. *New Phytol.* **214**, 879–889 (2017).
33. Selmecki, A. M. et al. Polyploidy can drive rapid adaptation in yeast. *Nature* **519**, 349–352 (2015).
34. Van de Peer, Y., Mizrahi, E. & Marchal, K. The evolutionary significance of polyploidy. *Nat. Rev. Genet.* **18**, 411–424 (2017).
35. Huysman, M. J. et al. Genome-wide analysis of the diatom cell cycle unveils a novel type of cyclins involved in environmental signaling. *Genome Biol.* **11**, R17 (2010).
36. Armbrust, E. V. The life of diatoms in the world's oceans. *Nature* **459**, 185–192 (2009).
37. Yahya, G. et al. Sublinear scaling of the cellular proteome with ploidy. *Nat. Commun.* **13**, 6182 (2022).
38. Sharpe, S. C. et al. Influence of cell size and DNA content on growth rate and photosystem II function in cryptic species of *Ditylum brightwellii*. *PLoS ONE* **7**, e52916 (2012).
39. Richard, W. Temperature and phytoplankton growth in the sea. *Fish. Bull.* **70**, 1063–1085 (1972).
40. Galitski, T., Saldanha, A. J., Styles, C. A., Lander, E. S. & Fink, G. R. Ploidy regulation of gene expression. *Science* **285**, 251–254 (1999).
41. Comai, L. The advantages and disadvantages of being polyploid. *Nat. Rev. Genet.* **6**, 836–846 (2005).
42. Quinton, R. J. et al. Whole-genome doubling confers unique genetic vulnerabilities on tumour cells. *Nature* **590**, 492–497 (2021).
43. Park, J. M. & Forsburg, S. L. Analysis of transcriptional response in haploid and diploid *Schizosaccharomyces pombe* under genotoxic stress. *G3: Genes, Genom., Genet.* **14**, jkae177 (2024).
44. Conant, G. C. & Wolfe, K. H. Turning a hobby into a job: how duplicated genes find new functions. *Nat. Rev. Genet.* **9**, 938–950 (2008).
45. Hirsch, S., Baumberger, R. & Grossniklaus, U. Epigenetic variation, inheritance, and selection in plant populations. *Cold Spring Harb. Symp. Quant. Biol.* **77**, 97–104 (2012).
46. McCaw, B. A., Stevenson, T. J. & Lancaster, L. T. Epigenetic responses to temperature and climate. *Integr. Comp. Biol.* **60**, 1469–1480 (2020).
47. Andalisi, A. A. et al. Defects arising from whole-genome duplications in *Saccharomyces cerevisiae*. *Genetics* **167**, 1109–1121 (2004).
48. Koester, J. A. et al. Sexual ancestors generated an obligate asexual and globally dispersed clone within the model diatom species *Thalassiosira pseudonana*. *Sci. Rep.* **8**, 10492 (2018).
49. Chao, D. et al. Polyploids exhibit higher potassium uptake and salinity tolerance in *Arabidopsis*. *Science* **341**, 658–659 (2013).
50. Wu, S. et al. Polyploidy in invasive *Solidago canadensis* increased plant nitrogen uptake, and abundance and activity of microbes and nematodes in soil. *Soil Biol. Biochem.* **138**, 107594 (2019).
51. Durkin, C. A., Mock, T. & Armbrust, E. V. Chitin in diatoms and its association with the cell wall. *Eukaryot. Cell* **8**, 1038–1050 (2009).
52. Martin-Jézéquel, V., Hildebrand, M. & Brzezinski, M. A. Silicon metabolism in diatoms: implications for growth. *J. Phycol.* **36**, 821–840 (2000).
53. Liu, S. et al. The *Brassica oleracea* genome reveals the asymmetrical evolution of polyploid genomes. *Nat. Commun.* **5**, 3930 (2014).
54. Song, Q. & Chen, Z. J. Epigenetic and developmental regulation in plant polyploids. *Curr. Opin. Plant Biol.* **24**, 101–109 (2015).

Publisher's note Springer Nature remains neutral with regard to jurisdictional claims in published maps and institutional affiliations.

Springer Nature or its licensor (e.g. a society or other partner) holds exclusive rights to this article under a publishing agreement with the author(s) or other rightsholder(s); author self-archiving of the accepted manuscript version of this article is solely governed by the terms of such publishing agreement and applicable law.

© The Author(s), under exclusive licence to Springer Nature Limited 2025

Methods

Ancestor strain

The marine diatom *Thalassiosira pseudonana* ((Hustedt) Hasle and Heimdal, CCMP 1335) was obtained from the Bigelow National Center for Marine Algae and Microbiota and had been in culture in our lab for about 2 years at the start of this experiment. Purified clones were obtained by spreading diluted stock cultures onto EASW medium agar plates; a single clone was chosen at random in October 2017. This clone initiated the ancestor or progenitor population for this experiment, which was maintained on EASW medium agar plates at 20.0 °C under a continuous photon flux density of ~20 μmol m⁻² s⁻¹. The median cell volume of this population was 45 μm³ as determined by a Z2 Coulter Counter (Beckman Coulter) with Coulter Z2 AccuComp software in November 2017. The particle counter provides an estimate of cell volume from an equivalent spherical diameter from a measure of conductivity. The cell volume was determined from the median of the distribution of tens of thousands of measurements. All phenotypic lines for this experiment originated from this ancestor population initiated from a single cell.

Isolation of phenotypic lines on the basis of cell volume

From late May to July in 2018, individual cultures of *T. pseudonana* were maintained in exponential phase under a series of temperatures (6.0, 10.0, 13.0, 15.0, 20.0, 25.0, 26.5, 27.5 and 28.5 °C) with a continuous photon flux density of 100 μmol m⁻² s⁻¹ using a semi-continuous batch technique (Fig. 1a). In a few of the temperature treatments (27.5 °C on 23 July, 6 °C on 30 July and 26.5 °C on 12 July), a small proportion of the population was composed of larger cells with double the expected cell volume (according to a histogram of cell volumes obtained from a Coulter counter). When the Coulter counter measurements detected any larger cells with double the expected cell volume within the population in an experimental bottle, a subculture was initiated and maintained in semi-continuous batch culture.

The newly established culture lines included ~45 μm³ cells and cells with enlarged cell volumes. These cultures with enlarged cells originated from cultures grown at temperatures warmer and colder than the optimal temperature for growth (23.3 °C) for the ancestral line; therefore, we hypothesized that cell enlargement might be important for thermal adaptation. Starting on 23 July we began subculturing these three lineages with enlarged cells and the ancestor line under a control temperature of 20.0 °C and an elevated temperature of 28.5 °C. We named these lines following the order of their discovery: control for the ancestral population grown at 20.0 °C, line 1 for the population with enlarged cells originating from the 26.5 °C culture, line 2 originating from the 27.5 °C culture and line 3 originating from the 6 °C culture. Since our initial goal was simply to maintain these new populations, and because this was an experiment based on a sudden discovery rather than one that was pre-designed, we did not establish multiple replicates of each line from the start, and the different lineages were subcultured in the 20.0 and 28.5 °C temperature treatments at different times. We monitored the growth rate and cell volume in all four lineages. When we transferred these lineages to 20.0 °C, line 2 had become dominated by enlarged cells with a greatly increased median cell volume, and the median cell volume differed between the 20.0 °C and 28.5 °C treatments at the start of the evolutionary experiment for all four lines (Fig. 1b and Table 1) due primarily to changes in the relative proportion of typically sized and enlarged cells within the lines. After 500 generations of cultivation, we confirmed that the cells in the control line had half the DNA content (the measurement of the DNA content can be seen in the ‘Genome-size measurement’ section of Methods) of cells in each of lines 1, 2 and 3. On the basis of these data, we inferred that the control line (small-sized phenotype) was diploid⁵⁵ (termed ‘D’) and the bigger phenotypes were tetraploids (termed ‘T1’, ‘T2’ and ‘T3’; Table 1 and Fig. 1c).

The selection experiment

Starting from 23 July, each phenotypic line was subcultured in a single bottle and underwent a temperature selection experiment for approximately 500 generations at 20.0 °C and 28.5 °C, with the start times of the experiments for different phenotypic lines not being exactly the same due to the varying times at which the cell enlargement phenomenon was observed (Fig. 1a). Twenty degrees Celsius was chosen as the control temperature because it was moderately lower than the ancestral strain’s optimal growth temperature, and 28.5 °C was chosen because it was close to the ancestral strain’s upper thermal limit. The start of growth for each phenotypic line under 20.0 °C and 28.5 °C is referred to as generation 0.

Each phenotypic line was maintained in a single 50 ml polycarbonate bottle in modified EASW medium⁵⁶, with pH 8.1 and a continuous photon flux density of 100 μmol m⁻² s⁻¹ in the bottle. Temperatures were maintained using growth chambers (Conviron A1000, Conviron). Cultures were manually agitated daily four or five times to reduce cell sedimentation. All phenotypic lines were maintained in semi-continuous batch culture and transferred during the exponential phase (maximum final cell densities did not exceed 5 × 10⁵ cells ml⁻¹). At 100 and 500 generations, each phenotypic line was transferred to four 1 l polycarbonate bottles for each temperature treatment for physiological parameters measurements and were sampled after 3 or 4 days of growth. The initial inoculation density was ranged from 35 to 200 cells ml⁻¹, adjusted according to the expected growth rates of different phenotypic lines at each temperature.

Growth and cell-size measurement

Cell density and median cell volume were monitored using a Z2 Coulter Counter (Beckman Coulter) with Coulter Z2 AccuComp software. The specific growth rates (μ) and the number of generations per transfer (G) were calculated as $\mu = \ln(C_{t_1}/C_{t_0})/\Delta t$ and $G = \Delta t / \left(\frac{\ln(2)}{\mu} \right)$, where μ is the specific growth rates (d⁻¹), C_{t_1} is the cell density at the end of the transfer, C_{t_0} is the inoculation cell density, and Δt is the elapsed time in days ($t_1 - t_0$).

Genome-size measurement

Genome size was estimated after 500 generations following ref. 57 with some modifications: briefly, 15 ml of mid-exponential cultures (~1 × 10⁵ cells ml⁻¹) was harvested by centrifugation, and pigments and RNA were then removed by ice-cold methanol and RNase A, respectively. Cells were then stained with SYBR Green I and analysed using the BD Accuri C6 Plus flow cytometer (BD Bioscience) and BD Accuri C6 Plus software (BD Bioscience). Note that this measurement was conducted only at 500 generations as ploidy analysis was not part of the original experimental design.

Photochemical traits

When cells were grown to 100 and 500 generations, the maximum quantum yield of PSII photochemistry (F_v/F_m), the functional absorption cross section of PSII (σ_{PSII}), the components in the relaxation kinetics of the fluorescence yield following the single turnover flash (alp3) and the non-photochemical quenching (NPQ) were measured by a fluorescence induction and relaxation system (FIRE, Satlantic). Excitation was achieved using a high-luminosity blue light-emitting diode (LED) array (455 ± 20 nm). PSII photochemistry parameters were determined by fitting the biophysical (KPF) model of ref. 58 to each fluorescence transient using the FIREPRO 4.3 software provided by Satlantic. Twenty to 30 replicate measurements were made on a sample and averaged. The PSII operating efficiency under actinic light Φ_{PSII} was calculated according to ref. 59, and NPQ was calculated according to ref. 60 as follows:

$$\Phi_{PSII} = (F'_m - F'_s)/F'_m$$

$$NPQ = (F_m - F'_m)/F'_m$$

where F_m is the maximum fluorescence, $F_{m'}$ is the maximum fluorescence under actinic light equivalent to the growth irradiance and F_s is the steady-state fluorescence at the growth irradiance.

For chlorophyll and carotenoid measurements, cultures (20 ml) were filtered onto Whatman GF/F membranes (effective pore size ~0.7 µm) under gentle vacuum pressure (<18 kPa or 5 inches Hg) and low light, followed by an overnight extraction with 90% acetone in the dark at 4 °C. Samples were then centrifuged at 4,300g, 4 °C for 10 min. The absorption of the supernatant was measured at 480, 630, 664 and 750 nm using a visible ultraviolet spectrophotometer (Shimadzu UV-2700). The chlorophyll *a* content was calculated following ref. 61. Total carotenoid content was calculated following ref. 62. Additional details are provided in our previous publication that characterizes the photochemical traits of *T. pseudonana* in response to environmental stressors⁶³.

Relative competitive fitness

The relative competitive fitness between D, T1, T2 and T3 was tested in exponentially growing co-cultures after ~100 and ~500 generations of selection at 20.0 °C and 28.5 °C if the cell sizes of the phenotype pairs could be clearly differentiated using the Z2 Coulter Counter. Cell density was monitored using a Z2 Coulter Counter (Beckman Coulter) with Coulter Z2 AccuComp software. At 100 generations, co-culture experiments were conducted using equal initial cell concentrations (50 cells ml⁻¹) of the different-sized population pairs (T2 and D; T3 and D; T2 and T1; and T3 and T1). After 500 generations of temperature selection, pre-experimental work established that the T1, T2 and T3 lineages would each dominate the D population in co-cultures after a single transfer when an equal cell ratio of the lineages was used as the initial inoculum. Therefore, an initial ratio of 10/1 (500 cells ml⁻¹ of the small lineage and 50 cells ml⁻¹ of the larger lineage) was used. Each co-culture competition experiment was conducted in triplicate. These experiments were run until one lineage reached at least 80% of the total cell abundance. The longest experiment ran ~200 generations. The relative competitive fitness was calculated as the growth rates ratio ($\mu_{\text{large}}/\mu_{\text{small}}$) between co-cultured lineages, where μ_{large} and μ_{small} represent the growth rates of the larger and smaller lineages, respectively. The specific growth rate was calculated as described earlier.

Thermal response of growth

The thermal reaction norm of the ancestor population was determined from estimates of acclimated exponential growth rate under nine temperatures (6.0, 10.0, 13.0, 15.0, 20.0, 25.0, 26.5, 27.5 and 28.5 °C) with a continuous photon flux density of 100 µmol m⁻² s⁻¹ in triplicate. After 500 generations of selection, the four lineages (D, T1, T2 and T3) that had been maintained under 20.0 °C and 28.5 °C were grown under thirteen temperatures (10.0, 12.1, 14.2, 16.4, 18.5, 20.0, 23.0, 25.5, 27.5, 28.5, 29.3, 31.3 and 33.4 °C) under continuous photon flux density of 100 µmol m⁻² s⁻¹. The assays were conducted using a custom-built temperature gradient block made of thermally conductive metal and connected to a circulating water-bath system. Twelve fixed positions were arranged along the gradient to hold culture vessels, creating 12 discrete temperature points. As the set-up supports 12 temperatures per run, the experiment was conducted in 2 consecutive batches to cover all 13 temperatures. All lineages were subcultured under each of the experimental temperatures for ~15 generations for pre-acclimation. Culture density was estimated by a Z2 Coulter Counter (Beckman Coulter) with Coulter Z2 AccuComp software.

We derived temperature-dependent trait values by fitting a model that estimated the optimal growth temperature (T_{opt}) on the basis of the temperature-dependent trait model described in ref. 64 and reformulated to explicitly include T_{opt} in ref. 9:

$$\mu = \frac{d_1 d_2}{b_2} e^{b_2 T + (d_2 - b_2) T_{\text{opt}}} - (d_0 + d_1 e^{d_2 T})$$

where μ is the specific growth rate (d⁻¹), T is temperature (°C), T_{opt} is the optimal growth temperature, d_1 is a pre-exponential constant for death, b_2 and d_2 are the exponential rates for birth and death, and d_0 is the temperature-independent death rate.

Transcriptome analysis

For transcriptomic analysis, the four lineages (D, T1, T2 and T3) that were grown under 20.0 °C and 28.5 °C for 100 and 500 generations were subcultured into four replicate bottles (4 phenotypic lines × 2 temperatures × 2 generation points (at 100 and 500 generations) × 4 replicates = 64 samples) and then collected in exponential phase by gentle filtration onto polycarbonate Millipore membrane filters (pore size 0.8 µm, diameter 25 mm). These samples were then immediately frozen in liquid nitrogen and stored at -80 °C until extraction. Total RNA was extracted using TRIzol reagent (Invitrogen) and RNeasy Plus Mini Kit (Qiagen) following the procedures described in previous studies^{65,66}. Briefly, a gDNA eliminator column (RNeasy Plus Mini Kit) and Qiagen's RNase-free DNase Set (an on-column treatment) were used to remove gDNA according to the manufacturer's instructions. RNA samples were then sequenced by Illumina HiSeq 6000 at the Genome Québec Innovation Centre with an Illumina TruSeq Stranded mRNA Library preparation method (paired-end 100 bp reads). All raw read files (detailed descriptions of these files are provided in Supplementary Dataset 1) are available through NCBI SRA (BioProject PRJNA1244923).

The quality and contamination of the raw reads were checked using FASTQC v0.11.9⁶⁷ and FastQ Screen v0.13.0⁶⁸ and inspected using MultiQC⁶⁹. Trimmomatic v0.39⁷⁰ with parameters set at ILLUMINACLIP:TruSeq3-PE.fa:2:30:10, LEADING:3, TRAILING:3, MINLEN:41, AVGQUAL:20, SLIDINGWINDOW:4:15 and HEADCROP:11 was used to remove low-quality bases and adaptor sequences of reads. Trimmed reads were mapped to *Thalassiosira pseudonana* CCMP1335 genome (NCBI, assembly ASM14940v2) to generate SAM files using HISAT2 v2.2.1⁷¹. SAM files were sorted and converted to BAM files using SAMTOOLS v1.13⁷². Gene expression in transcripts per million was calculated from BAM files using STRINGTIE v2.2.1⁷³. A gene count matrix was generated from STRINGTIE gtf results using the prepDE.py script. Differential expression was calculated between the polyploid lineages and the diploid lineage under the same temperature and generation number using gene count matrix data using DESeq2 v1.42.0⁷⁴. Genes with a Benjamini–Hochberg adjusted *P* value < 0.01 (Supplementary Dataset 2) were considered as DEGs.

Gene expression analyses

We assessed the variation in gene expression across replicates, lineages, temperatures and number of generations using a principal component analysis on transcript counts. The amount of differential expression was assessed by counting the number of DEGs and the distribution of log₂ fold change of the DEGs in each polyploid relative to the diploid at each temperature after 100 and 500 generations. We counted the DEGs for each polyploid line at each temperature treatment at 100 and 500 generations (Supplementary Dataset 3).

For each temperature treatment at 100 and 500 generations, we identified and counted GO-bp terms enriched in up- or down-regulated genes common to all three polyploids (pDEGs). We repeated the gene enrichment analyses on up- and down-regulated genes for each of the following pairs of conditions: the same temperature (20.0 or 28.5 °C) at both 100 and 500 generations; 100 and 500 generations and both experimental temperatures. There were so few genes up- or down-regulated across all polyploids under both 20.0 and 28.5 °C that we could not do an enrichment analysis on this small subset of genes. Detailed heat maps of the log₂ fold change of genes within the enriched GO-bp super classes, and additional KO terms of interest, are provided in Supplementary Dataset 4. Data analysis and visualizations were made using R v.4.0.2⁷⁵, packages ggplot2 v.3.2.0⁷⁶ and Pheatmap v.1.0.12⁷⁷.

Enrichment analysis

We performed a GO enrichment analysis to test for overrepresentation of GO-bp terms within the input gene sets (the pDEGs) through a hypergeometric test from GOstats v. 2.62.0⁷⁸ R package with a Benjamini–Hochberg adjusted *P*-value cut-off of 0.01. REViGO⁷⁹ (<http://revigo.irb.hr>) was used to remove redundant and similar GO-bp terms to yield a smaller number of categories by semantic clustering.

Statistical analyses

Four biological replicates were sampled at 100 and 500 generations, respectively. Three independent lines were used for the co-culture competitive experiments. Thermal reaction norms were performed using three independent biological replicates. A Mann–Whitney *U* test was used to test whether |log₂FC| values of DEGs of polyploid lines between different treatments are associated with significant differences. One-way analysis of variance was used to determine whether lineages were associated with significant differences in physiological parameters. Statistical analyses were all carried out using R v.4.0.2⁷⁵.

Data availability

The data are available in the Supplementary Information of this article and via figshare at <https://doi.org/10.6084/m9.figshare.28738802> (ref. 80). The sequencing data of RNA-seq of this study are available through NCBI SRA (BioProject: PRJNA1244923). Source data are provided with this paper.

Code availability

The R code for generating the figures in this work is available via figshare at <https://doi.org/10.6084/m9.figshare.28738802> (ref. 80).

References

55. Armbrust, E. V. et al. The genome of the diatom *Thalassiosira pseudonana*: ecology, evolution, and metabolism. *Science* **306**, 79–86 (2004).
56. Berges, J. A., Franklin, D. J. & Harrison, P. J. Evolution of an artificial seawater medium: improvements in enriched seawater, artificial water over the last two decades. *J. Phycol.* **37**, 1138–1145 (2001).
57. Smith, S. R. et al. Transcript level coordination of carbon pathways during silicon starvation-induced lipid accumulation in the diatom *Thalassiosira pseudonana*. *New Phytol.* **210**, 890–904 (2016).
58. Kolber, Z. S., Prášil, O. & Falkowski, P. G. Measurements of variable chlorophyll fluorescence using fast repetition rate techniques: defining methodology and experimental protocols. *Biochim. Biophys. Acta* **1367**, 88–106 (1998).
59. Genty, B., Briantais, J. M. & Baker, N. R. The relationship between the quantum yield of photosynthetic electron transport and quenching of chlorophyll fluorescence. *Biochim. Biophys. Acta* **990**, 87–92 (1989).
60. Bilger, W. & Björkman, O. Role of the xanthophyll cycle in photoprotection elucidated by measurements of light-induced absorbance changes, fluorescence and photosynthesis in leaves of *Hedera canariensis*. *Photosynth. Res.* **25**, 173–185 (1990).
61. Jeffrey, S. T. & Humphrey, G. F. New spectrophotometric equations for determining chlorophylls *a*, *b*, *c1* and *c2* in higher plants, algae and natural phytoplankton. *Biochem. Physiol. Pflanz.* **167**, 191–194 (1975).
62. Davies, B. H. Chemistry and biochemistry of plant pigments. *Carotenoids* **2**, 38–165 (1976).
63. Li, Z. et al. Dynamic photophysiological stress response of a model diatom to ten environmental stresses. *J. Phycol.* **57**, 484–495 (2021).
64. Thomas, M. K. et al. Temperature–nutrient interactions exacerbate sensitivity to warming in phytoplankton. *Glob. Change Biol.* **23**, 3269–3280 (2017).
65. Li, Z., Zhang, Y., Li, W., Irwin, A. J. & Finkel, Z. V. Common environmental stress responses in a model marine diatom. *New Phytol.* **240**, 272–284 (2023).
66. Li, Z., Zhang, Y., Li, W., Irwin, A. J. & Finkel, Z. V. Conservation and architecture of housekeeping genes in the model marine diatom *Thalassiosira pseudonana*. *New Phytol.* **234**, 1363–1376 (2022).
67. Andrews, S. *FastQC: A Quality Control Tool for High Throughput Sequence Data*. (Babraham Bioinformatics, Babraham Institute, 2010).
68. Wingett, S. W. & Andrews, S. FastQ Screen: a tool for multi-genome mapping and quality control. *F1000Res.* **7**, 1338 (2018).
69. Ewels, P., Magnusson, M., Lundin, S. & Käller, M. MultiQC: summarize analysis results for multiple tools and samples in a single report. *Bioinformatics* **32**, 3047–3048 (2016).
70. Bolger, A. M., Lohse, M. & Usadel, B. Trimmomatic: a flexible trimmer for Illumina sequence data. *Bioinformatics* **30**, 2114–2120 (2014).
71. Kim, D., Langmead, B. & Salzberg, S. L. HISAT: a fast spliced aligner with low memory requirements. *Nat. Methods* **12**, 357–360 (2015).
72. Li, H. et al. The sequence alignment/map format and SAMtools. *Bioinformatics* **25**, 2078–2079 (2009).
73. Pertea, M. et al. StringTie enables improved reconstruction of a transcriptome from RNA-seq reads. *Nat. Biotechnol.* **33**, 290–295 (2015).
74. Love, M. I., Huber, W. & Anders, S. Moderated estimation of fold change and dispersion for RNA-seq data with DESeq2. *Genome Biol.* **15**, 550 (2014).
75. R Core Team *R: A Language and Environment for Statistical Computing* (R Foundation for Statistical Computing, 2013).
76. Wickham, H. *ggplot2: Elegant Graphics for Data Analysis* (Springer, 2016).
77. Kolde, R. *Pheatmap: pretty heatmaps Version 1.0.12* (2019); <https://CRAN.R-project.org/package=pheatmap>
78. Falcon, S. & Gentleman, R. Using GOstats to test gene lists for GO term association. *Bioinformatics* **23**, 257–258 (2007).
79. Supek, F., Bošnjak, M., Škunca, N. & Šmuc, T. REViGO summarizes and visualizes long lists of gene ontology terms. *PLoS ONE* **6**, e21800 (2011).
80. Li, Z. et al. Supporting data for ‘Polyploidization in diatoms accelerates adaptation to warming’. figshare <https://doi.org/10.6084/m9.figshare.28738802> (2025).

Acknowledgements

This work was supported by the National Natural Science Foundation of China (32371681 and 32001180 (Z.L.)), the Natural Sciences and Engineering Research Council of Canada (NSERC) Discovery (Z.V.F., A.J.I.), Canada Research Chairs (Z.V.F.) programme and the Simons Collaboration on Computational Biogeochemical Modeling of Marine Ecosystems/CBIOMES (grant ID 549937 (Z.V.F.) and 549935 (A.J.I.)).

Author contributions

Z.L. and Z.V.F. designed the research. Z.L. and Y.Z. performed the experiments, Z.L. performed the bioinformatics analysis, Z.L., A.J.I. and Z.V.F. wrote the paper, and all authors contributed to the corrections of the paper.

Competing interests

The authors declare no competing interests.

Additional information

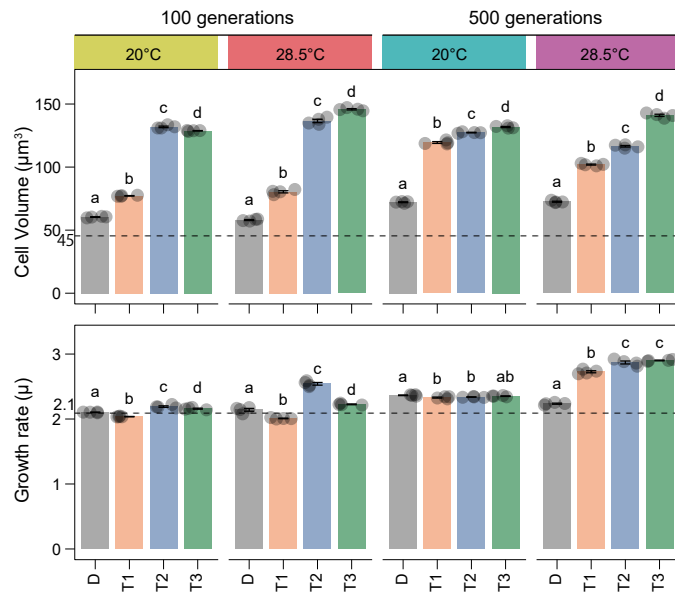
Extended data is available for this paper at <https://doi.org/10.1038/s41558-025-02464-1>.

Supplementary information The online version contains supplementary material available at <https://doi.org/10.1038/s41558-025-02464-1>.

Correspondence and requests for materials should be addressed to Zhengke Li.

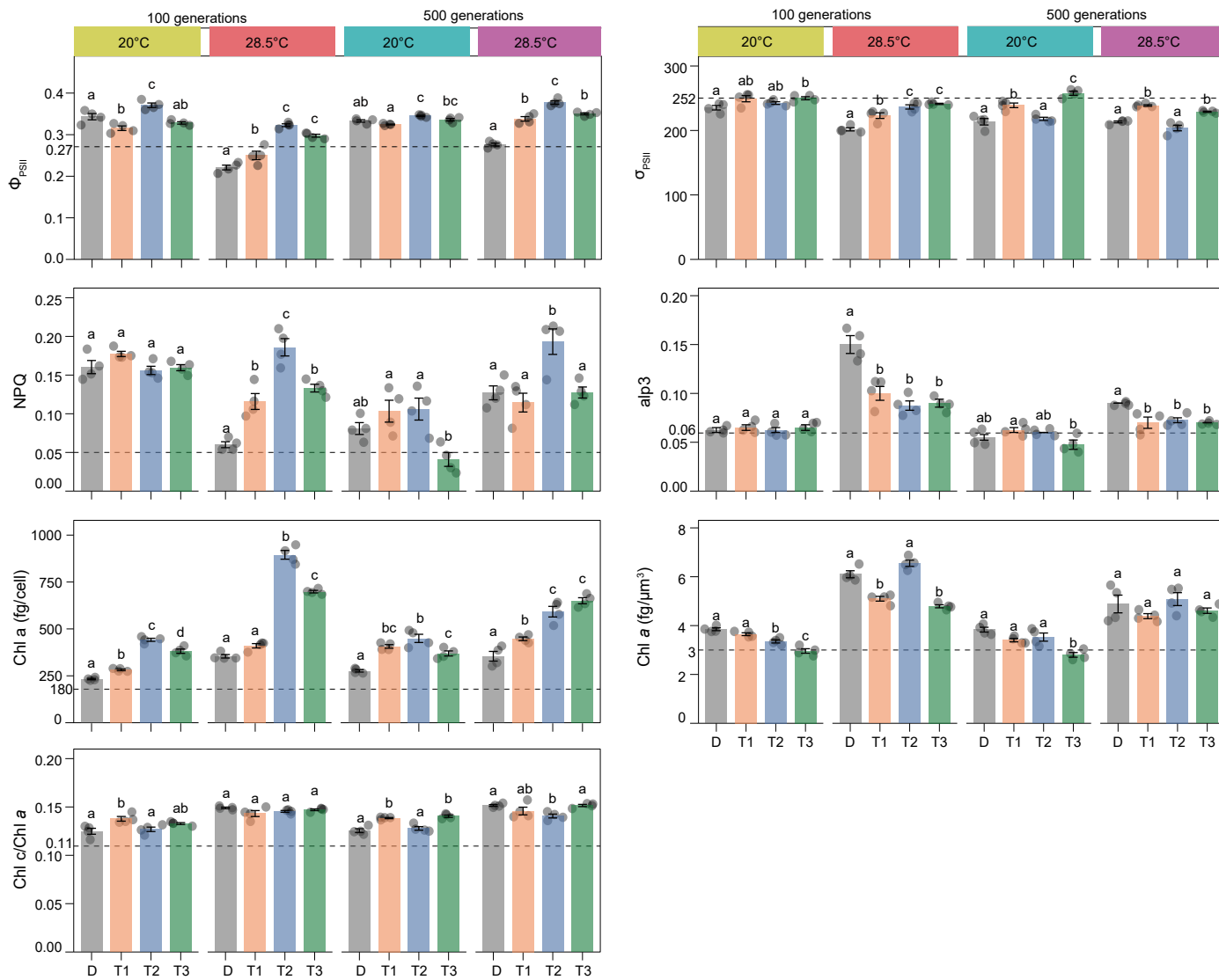
Peer review information *Nature Climate Change* thanks María Aranguren-Gassis, Gwenn Hennon, Peng Jin and Conny Sjöqvist for their contribution to the peer review of this work.

Reprints and permissions information is available at www.nature.com/reprints.



Extended Data Fig. 1 | Cell volume and growth rate of polyploid and diploid lineages after 100 and 500 generations of temperature selection (20 °C and 28.5 °C). The horizontal dotted line is a value for the ancestral at 20 °C. Bars with different superscript letters for each combination of generation

and temperature treatment indicate significant differences (One-way ANOVA with two-sided Tukey's HSD, $P < 0.05$). Data are means \pm SD ($n = 4$ biological replicates). D: Diploid control line; T1: Tetraploid lineage 1; T2: Tetraploid lineage 2; T3: Tetraploid lineage 3.



Extended Data Fig. 2 | Photophysiological parameters of polyploid and diploid lineages after 100 and 500 generations of temperature selection (20 °C and 28.5 °C). Φ_{PSII} : the PSII operating efficiency; σ_{PSII} : the functional absorption cross section of PSII; NPQ: the non-photochemical quenching; alp3: the components in the relaxation kinetics of the fluorescence yield following the single-turnover flash; Chl a (fg/ μm^3): the chlorophyll a content per cell volume; Chl a (fg/cell): the chlorophyll a content per cell; Chl c /Chl a : the chlorophyll

c to chlorophyll a ratio. The horizontal dotted line is a value for the ancestral at 20 °C. Bars with different superscript letters for each combination of generation and temperature treatment indicate significant differences (One-way ANOVA with two-sided Tukey's HSD, $P < 0.05$). Data are means \pm SD ($n = 4$ biological replicates). D: Diploid control line; T1: Tetraploid lineage 1; T2: Tetraploid lineage 2; T3: Tetraploid lineage 3.